Simulated Bombardment of Diamond With Hydrogen Isotopes

James A. Pittard, Mikhail Y. Lavrentiev, and Neil A. Fox

***Abstract*— Diamond is a material of interest for windows, sensors, and even plasma facing materials (PFMs) within the first wall of fusion reactors. As with any material within the first wall, both fuel retention and hydrogen etching must be considered. In order to develop understanding of diamond's interaction with hydrogen in fusion relevant conditions, a series of repeated single bombardment molecular dynamics simulations have been performed. The impact of incident hydrogen mass, energy, and incident angle, as well as the diamond temperature and orientation were all explored. It was found that vacancy formation was restricted to the top unit cell (UC), (110) and (111) surfaces exhibited a notable decrease in vacancies compared with (100), and reflection of incident atoms was largely dictated by the atom's vertical momentum. In general, in the case of pristine diamond, changes in surface orientation and temperature appear to have minimal impact on retention. However, both these variables did affect vacancy formation, suggesting they could become significant as the surface becomes damaged.**

***Index Terms*— Diamond, fusion reactors, hydrogen, materials science and technology, modeling.**

I. Introduction

SELECTION of appropriate materials for the first wall of fusion reactors remains one of the biggest challenges facing the success of commercial fusion. Material requirements are also evolving due to the unique needs of demonstration tokamaks, spherical tokamaks, and other alternative designs making continuous material development vital. A common need among these different reactor designs is appropriate plasma facing materials (PFMs). Such materials must be able to withstand incredibly high thermal loads, strong magnetic fields, high-energy neutron fluxes, and an interaction with a hydrogen plasma, all while exhibiting minimal plasma contamination and fuel retention.

Diamond's exceptional thermal properties, low atomic number, radiation hardness, resistance to physical sputtering, and ability to withstand plasma contact make it a material of interest for various applications within the first wall [1], [2], [3], [4], [5], [6], [7], [8], [9]. However, as with previously used graphite tiles, carbon-based materials accompany concerns surrounding chemical etching and fuel retention. As such, a greater understanding of the interaction between diamond and hydrogenic species at fusion relevant conditions is required to assess these concerns.

Previous work determined deuterium retention of diamond as equivalent to metallic PFMs tested in the same setup [10]. In addition, molecular dynamics simulations suggested a two-step etching mechanism in which an initial swelling phase was required before the removal of carbon could be observed. In order to develop understanding of previous results and to influence future experiments, this study considers how different variables might impact hydrogen retention and the damage sustained by the diamond. To do this, a series of repeated single bombardment simulations have been carried out with large-scale atomic/molecular massively parallel simulator (LAMMPS) [11], [12]. Each simulation consisted of a block of diamond hit with a single hydrogen atom (hydrogen isotopes are collectively referred to as hydrogen throughout), which was then repeated a minimum of 300 times for each set of conditions. The mass, energy, and incident angle of bombarding hydrogen, as well as diamond orientation and temperature were all varied. The impact of such variables was evaluated through measurements of vacant sites, interstitial carbon, sputtered carbon, reflected hydrogen, and hydrogen positions.

II. Method

Simulations consisted of a diamond block of 5×5 unit cells (UCs) in area and a depth that was varied based on the expected implantation depth. Periodic boundary conditions in x- and y-dimensions and a finite boundary condition in z helped mimic a larger diamond block while allowing atoms to leave out the top of the simulation box. On the side opposite to the implantation surface, a 1 UC thick layer was frozen in place. This, combined with the periodic boundary conditions, prevents the diamond from shifting during implantation.

For each repeat, a hydrogen atom was created 3 UCs above the surface in a position that insured it was incident on the randomly generated target position by consideration of incident and planar angles (θ and φ, respectively; see Fig. 1). For nonzero θ, φ is randomly generated unless specific directions were used (such as $\langle 110 \rangle$ or $\langle 111 \rangle$). Random seeds in the input file were also regenerated for each repeat.

The (100) diamond blocks were constructed by replicating out an eight-atom UC. To create other orientations, a large

Manuscript received 29 September 2023; revised 2 July 2024; accepted 26 July 2024. Date of publication 8 August 2024; date of current version 9 December 2024. This work was supported in part by Engineering and Physical Sciences Research Council (EPSRC), in part by UK Atomic Energy Authority (UKAEA), and in part by Research Councils UK (RCUK) Energy Program under Grant EP/W006839/1. The review of this article was arranged by Senior Editor R. Chapman. *(Corresponding author: James A. Pittard.)*

James A. Pittard and Neil A. Fox are with the School of Physics, University of Bristol, BS8 1UB Bristol, U.K. (e-mail: jp17358@bristol.ac.uk; neil.fox@bristol.ac.uk).

Mikhail Y. Lavrentiev is with the Culham Campus, UKAEA, OX14 3DB Abingdon, U.K. (e-mail: mikhail.lavrentiev@ukaea.uk).

Color versions of one or more figures in this article are available at https://doi.org/10.1109/TPS.2024.3435521.

Digital Object Identifier 10.1109/TPS.2024.3435521

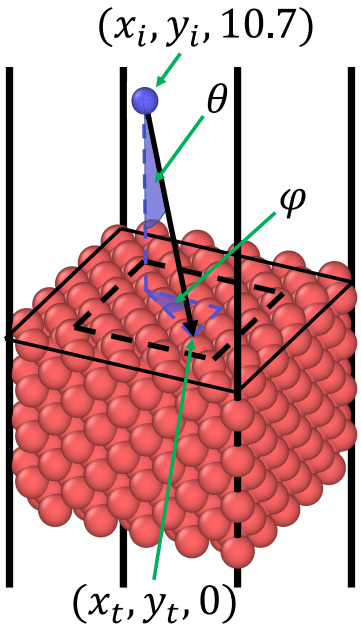

Fig. 1. Path of hydrogen atom (blue) at an incident angle, θ, toward a $5 \times 5 \times 4$ UC diamond block (red atoms). φ is the angle of implantation about the z-axis. A target location (x_t, y_t) is generated at random within a 3×3 central region (black dashed line). Initial position (x_i, y_i) is calculated, so the hydrogen atom hits the target position when created at a height of 3 UCs above the surface. Base diagram rendered in Ovito [13].

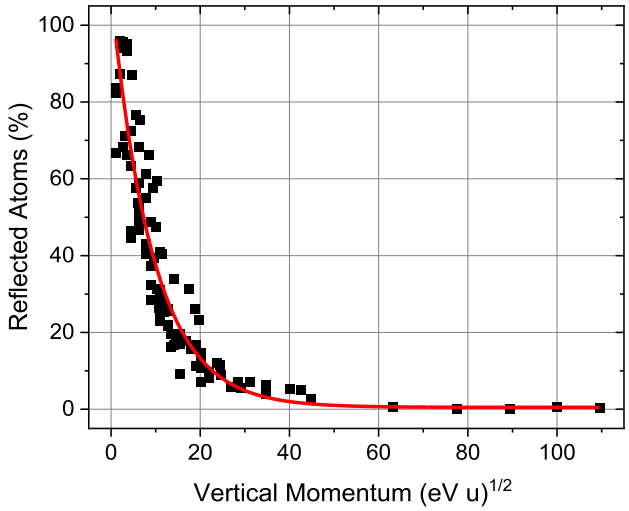

Fig. 2. Percentage of simulation repeats, which resulted in the reflection of the incident ion. A single ion was incident in each simulation; for a given set of conditions, a simulation was repeated 300 times. Incident angle, energy, and mass of implanted atoms were varied, as well as surface orientation and diamond temperature. Units of vertical momentum, P_z, have been selected for ease of conversion to energy, E, and mass, m, via $P_z = (2Em)^{1/2}\cos(\theta)$, where θ is the incident angle. Data have been fit with $y = y_0 + Ae^{-x/t}$, where $y_0 = 0.498 \pm 2.664\%$, $A = 107.9 \pm 3.9\%$, and $t = 9.4 \pm 0.8$ $(eVu)^{1/2}$.

(100) orientated block was created, a rotation matrix applied, and the rotated block was trimmed to the desired size—giving a flat surface of the desired orientation. An energy minimization was then performed on the trimmed, rotated block, and the relaxed structure is used as the data file for simulations. This method required larger surface areas of 8×8 UCs to ensure stability. A (100) block was also constructed in this manner (referred to as "(100) relaxed") to ensure that the method of construction was not impacting results.

Three different diamond temperatures (300, 600, and 1000 K) and four different diamond surfaces [(100), (100) relaxed, (110), and (111)] were tested. Hydrogen masses of one (protium), two (deuterium), three (tritium), and an unphysical mass ten were all tested. For every set of conditions, hydrogen energies of 10, 30, 60, and 100 eV were used; however, additional energies were also explored for some conditions with an overall range of 5–500 eV. Incident angle, θ, was varied between 0° and 85° with a random φ, as well as ⟨110⟩ and ⟨111⟩ directions.

The reactive empirical bond order (REBO) potential was used to dictate carbon–carbon and carbon–hydrogen interactions [14], [15]. All bombarding atoms were treated as hydrogen regardless of mass. Atoms outside of the frozen layer were given velocities sampled from a Gaussian distribution corresponding to the target temperature. Target temperature was maintained throughout simulations by sampling velocities from the NVT ensemble. A short temperature damping parameter of 0.1 ps was used to allow for a rapid return to target temperature post implantation. A variable timestep ensured atoms moved no more than 0.1 Å per timestep, with a default value of 0.5 fs. An initial run of 3 ps allowed the target temperature to stabilize before the bombarding atom hits the surface. Once the incident hydrogen had been created, the simulation was run for 10 ps, giving sufficient time for the atom to hit the surface and come to rest in a stable position. Following this, the temperature was reduced to 0 K to remove thermal movement to improve vacancy analysis accuracy.

The analysis performed looked to quantify the impact of variables concerning both the hydrogen and the diamond. Hydrogen was classified as either implanted or reflected. If there was no hydrogen in the simulation box, or it was at a height greater than 2 Å from the surface, it was considered to be reflected. Hydrogen within 2 Å of the surface was taken to be implanted.

A Wigner–Seitz analysis was used via the Ovito python package to determine vacancies and interstitials [13], [16]. The final output file (post bombardment, at a temperature of 0 K with hydrogen removed) was compared with the initial file, which acted as a reference. A Wigner–Seitz (or Voronoi) cell was constructed about each of the atomic sites. Using atom coordinates from the final output file, the occupancy of carbon atoms for each cell was determined. For cells with an occupancy of one, it was deemed that no point defect has occurred, whereas cells with occupancies of two or zero corresponded to interstitials and vacancies, respectively. Typically zero or one vacancy formed; as such, the percentage of simulations containing one or more vacancies was considered (referred to as "vacancy percentage"). Although sputtered atoms were counted (taken to be the difference between the number of interstitials and vacancies), values were very low, and no meaningful conclusions could be drawn from this data.

III. Results and Discussion

A. Reflected Atoms

As can be seen in Fig. 2, percentage of reflected particles was largely dictated by vertical angular momentum. Low vertical momentum can be a consequence of lower isotope

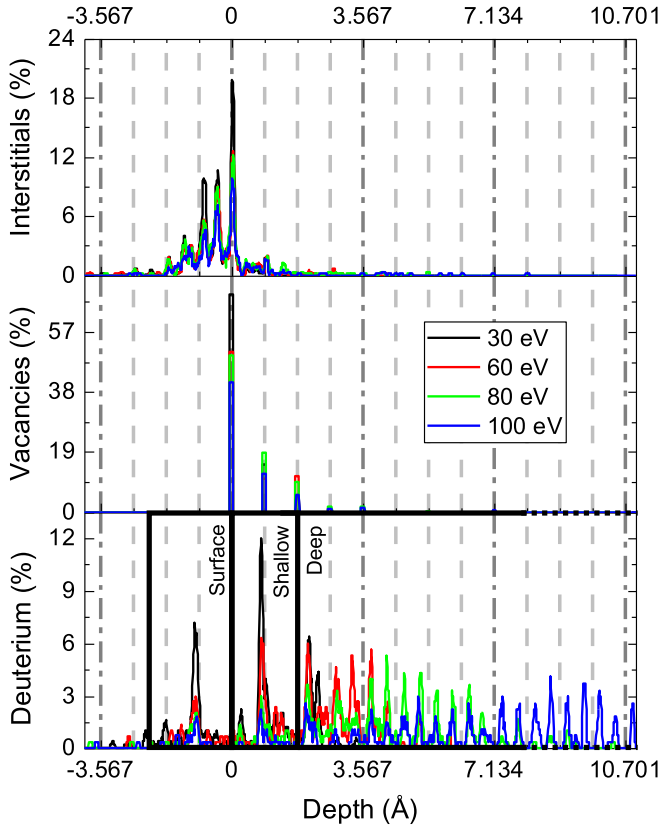

Fig. 3. Defect analysis of four datasets of 300 repeats of a (100) diamond block at 300 K being bombarded with a single deuterium atoms of 30, 60, 80, and 100 eV normal to the surface. *y*-axis units are as a percentage of incident atoms (for example, 39% of incident atoms caused a vacancy in the top AL for 100 eV). Interstitials are the depth of any carbon atom with an occupancy of two, meaning each vacant site will result in two interstitials provided no carbon is lost. The percentage was halved to account for this. Dashed lines show the ALs of the diamond, with markers at every UC. Three depth categories (*surface*, *shallow*, and *deep*) were used for discussion as marked on the deuterium density plot.

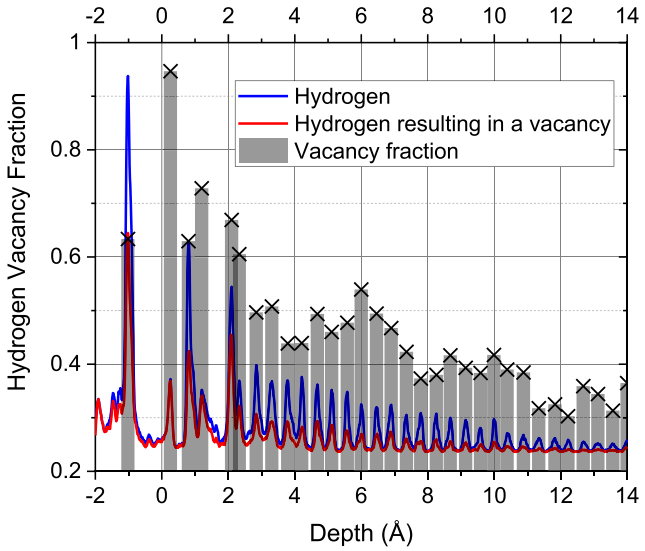

Fig. 4. Fraction of hydrogen that caused one or more vacancies compared with all implanted hydrogen as a function of depth for all simulations of a (100) surface. Blue line shows the density of hydrogen depths, and the red line also shows this but only for hydrogen that resulted in one of more vacancies forming. The black bars show the ratio between two densities for the hydrogen peaks.

mass, lower isotope energy, or an increased incident grazing angle. Increased vertical momentum increases the likelihood that an incident atom will continue into the diamond after collisions with carbon atoms and reduces the likelihood of it being reflected. As Fig. 2 shows data across all variables tested (different temperatures, incident angles, surfaces, and atom masses), it suggests that diamond temperature and orientation would have minimal impact on reflection. Although hydrogen retention is likely to be impacted by reflection, it would be expected that penetration depth and vacancy formation would also be significant. Higher depths result in a larger interaction volume, and more hydrogen can be taken up before saturation is reached [10]. In addition, damage sustained to the diamond could create new binding sites that would not be accessible in pristine diamond. As discussed later, both diamond temperature and orientation saw changes in vacancy formation and minor changes in average depth, suggesting an impact on retention could still be expected even if changes to reflection are negligible.

B. Vacancy Formation

Fig. 3 shows the depths of carbon interstitials, vacant sites, and implanted deuterium for four datasets of different energies. Regardless of energy, it can be seen that vacant sites are restricted to the top UC of the diamond block, despite the majority of higher energy deuterium residing beyond this region. Vacancies form readily in the top few atomic layers (ALs) where carbon atoms can be pushed out of the surface—as seen from the carbon interstitial positions. The deuterium does not have sufficient energy to produce vacancies deeper within the diamond where interstitial positions for the carbon are less readily available.

Fig. 4 shows the correlation between hydrogen depth and vacancy formation. As with Fig. 3, peaks in hydrogen density correspond to regions occupied by hydrogen within the diamond. The bars on Fig. 4 show the fraction of hydrogen in these locations that resulted in one of more vacancies forming ("vacancy fraction"). It can be seen that hydrogen occupying positions deeper within the diamond are less likely to have formed a vacancy. This is thought to be a result of vacancies only forming within the top ALs of the diamond, as shown in Fig. 3. Hydrogen retained within the surface layers can push carbon out of the surface, as suggested by the depth of interstitials in Fig. 3, whereas hydrogen retained deeper within the diamond is unable to significantly displace carbon deeper than the surface. In some cases, positions occupied by hydrogen appear to only become available when a vacancy has formed, and this seems likely for the peak at a depth of 0.2 Å, which gives a vacancy fraction of nearly 1, meaning practically no hydrogen occupied this depth without forming a vacancy. These new sites are only forming, and therefore occupied, near the surface, resulting in an increase in vacancy fraction. Lower vacancy fractions (~0.6) are also observed at depths at which vacancies can form, suggesting the lateral position of the hydrogen is impacting vacancy formation alongside depth. However, as some hydrogen is able to form a vacancy in the surface while coming to rest at a point beyond vacancy forming depths, vacancy formation cannot be solely dictated

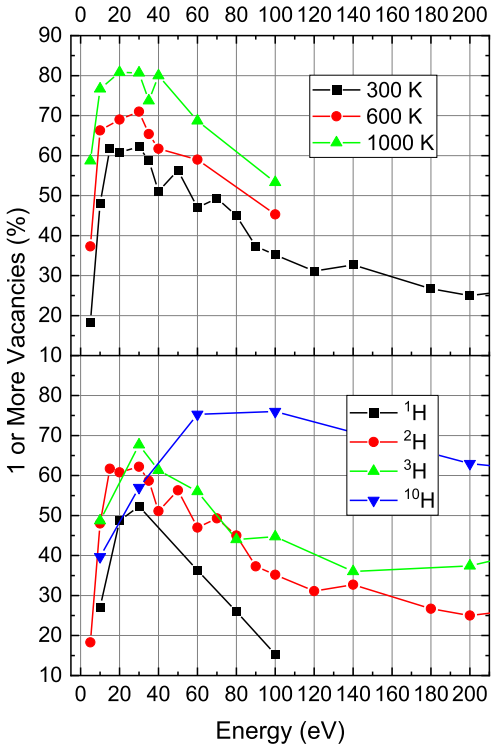

Fig. 5. Percentage of simulation repeats, which resulted in the formation of one or more vacancies for different diamond temperatures (top) and incident hydrogen masses (bottom). A single hydrogen was incident in each simulation; for a given set of conditions, a simulation was repeated 300 times. All simulations performed on a (100) surface with a 0° incident angle. Deuterium (^{2}H) was used for temperature variation, while mass variation used a diamond temperature of 300 K.

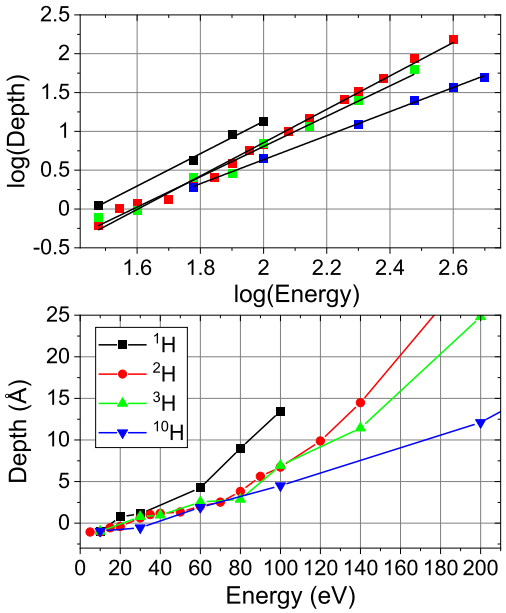

Fig. 6. Average depth for a series of repeated, single bombardment simulations of hydrogen isotopes of varying mass and energy at an incident angle of 0° on a (100) diamond surface at 300 K. Linear fits have been applied to the logarithmic plot giving gradients of ^{1}H: 2.08 ± 0.09, ^{2}H: 2.15 ± 0.05, ^{3}H: 1.95 ± 0.10, and ^{10}H: 1.55 ± 0.03.

by exact position, and the amount of energy transferred to surface atom in initial collisions must be of some importance.

At low energies, small increases in energy result in a significant increase in vacancy formation, as seen in Fig. 5.

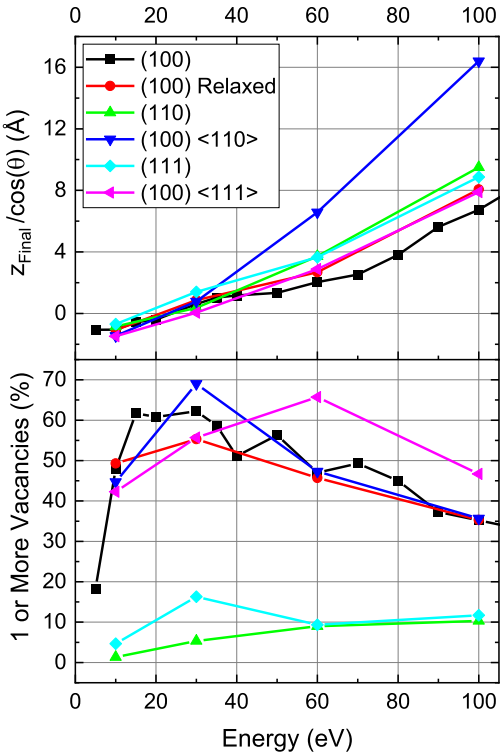

Fig. 7. Results from repeated simulations of deuterium bombarding various diamond surfaces at 300 K. Where only a surface is specified in legend, bombarding atoms were at an incident angle of 0°. Directions indicated correspond to implantation angles upon a (100) surface. (110), (111), and (100) relaxed were all constructed by applying a rotation matrix to a larger block of diamond, trimming it to size, and performing an energy minimization. The depth plotted takes into account the incident angle, θ, effectively plotting the distance traveled within the diamond rather than depth, z_{final}.

After peak vacancy formation is reached, a more gradual decrease is observed with increasing energy. Although the energy range of the initial increase in vacancy formation corresponds to the drop-off in reflected atoms seen in Fig. 2, it is not a result of decreased reflection. Reflected hydrogen contributes a significant amount to total vacancies formed, with 52% of reflected hydrogen resulting in a vacancy (across all simulations). This percentage was typically highest with higher energies, as reflection will more commonly occur from a head on collision, which is more likely to create a vacancy due to greater energy transfer. Instead, this increase is simply a result of some minimum energy required to create a vacancy, with the energy of vacancy formation reported at around 9–15 eV [17]. As discussed regarding Fig. 3, the gradual decrease is thought to be a result of the reduction in hydrogen retained within the first few ALs.

In Fig. 5, it can be seen that the energy at which peak vacancy formation occurs also increases with mass and shows a longer tail afterward. Reduced energy transfer between collisions [10] results in lighter masses traveling deeper into the diamond, as seen in Fig. 6. Deeper penetration depths correlate with reduced vacancy formation (see Fig. 4), so the drop-off in vacancies is faster for lower masses. These observations are in contrast to what is observed for temperature variation, where no change in the energy for peak vacancy formation was observed. However, an increase in temperature did result in

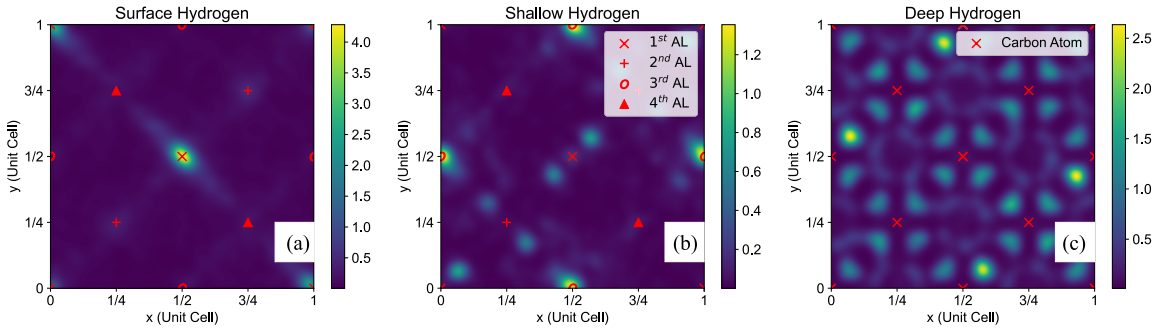

Fig. 8. Heat map of xy hydrogen positions within the UC at three different depth regions following repeated simulations of hydrogen bombardment. Values on color scale are arbitrary but indicate the density of hydrogen. Data were taken across all simulations of (100) surface orientations. Hydrogen with a final depth, z, of $-2 < z < 0$ Å was classified as surface hydrogen (a), $0 < z < (1/2)$ UC as shallow (b), and $z > (1/2)$ UC as deep (c). Red markers represent carbon atom positions. Where appropriate, different markers have been used to show the different ALs of the diamond.

an increase in vacancies. The higher average energy of carbon atoms meant they were more susceptible to displacement and vacancy formation.

A significant difference between the three surface orientations was observed in Fig. 7, with both (110) and (111) surfaces showing a notable reduction in vacancies formed compared with all (100) surfaces, including (100) relaxed. It is thought there are two reasons why these surfaces displayed lower vacancy formation. (111) has a significantly lower surface energy than (100) [18] and a higher displacement energy in this direction [19], giving a reduction in vacancies compared with (100). However, (110) has a surface energy very similar to (100) and a lower displacement energy and yet still displayed lower vacancy formation. Instead, the reduction is thought to be a result of atom alignment. In ⟨110⟩, clear channels can be observed, which reduce the chance of collision with carbon atoms in the top ALs and, therefore, vacancies. The same reduction was not observed for (100) in the ⟨110⟩ direction, as the 45° incident angle meant more of the collisions that occurred would have been in the top ALs.

C. Hydrogen Positions

Changes to the temperature and orientation of the diamond resulted in minimal changes in average depth, although small increases were observed for higher temperatures and the (110) surface. The higher temperature encourages movement of the carbon atoms, resulting in slightly increased penetration depths. As previously discussed, channels can be seen in the ⟨110⟩ direction, which could increase penetration depths. In fact, hydrogen incident in ⟨110⟩ on a (100) surface resulted in a significant increase in average penetration depth when incident angle was accounted for. This is likely to be impacted by the real depth being shallower and shallow hydrogen occupying different interstitial positions (see Fig. 3). However, it is still a notable increase on the ⟨111⟩ direction on a (100) surface, which had the same incident angle but different φ values—suggesting these channels are significant.

Parameters surrounding the incident hydrogen had a much greater impact than the diamond. Increasing energy of hydrogen resulted in a nonlinear increase in penetration depth. This relation is dominated by "sticking" to the surface at low energies (< 30 eV), and then, transitions to a relationship dictated by the mass but always greater than linear as seen in the gradients of the log plot in Fig. 6. This greater than linear behavior has been observed in simulations of other materials [20] and was attributed to channeling effects, which require modeling atomic structure explicitly, as is done in molecular dynamics. Hydrogen with sufficient energy to penetrate the first few ALs travels deeper into the crystal, as they travel through atomic channels within the crystal structure. For multiple bombardments, the greater than linear relation is expected to be exaggerated, as lower energy/depth hydrogen creates more vacancies and trapping sites near the surface, further reducing penetration at low energies.

A more detailed look into interstitial positions occupied by the hydrogen was also carried out. Hydrogen depths seen in Fig. 3 were considered in three regions: surface hydrogen within 2 Å of the surface, shallow hydrogen at a depth between 0 and (1/2) UC, and deep hydrogen at depths greater than this. The xy positions of hydrogen with respect to the UC were plotted for each depth selection, as seen in Fig. 8. Surface hydrogen is positioned directly above atoms on the top AL, as seen in Fig. 8(a). The shallow hydrogen in Fig. 8(b) mostly occupies positions in midpoints between atomic sites in the third AL and the tetrahedral positions on the first/surface AL (a C-site [21]). This occupation is only observed for shallow hydrogen, at a depth where there are no carbon atoms directly above this position. For deep hydrogen, there are carbon atoms above this position, which seems to make its occupation energetically unfavorable, as different positions are occupied. Other positions, more similar to those observed for deep hydrogen, are also present at shallow depths but to a lesser extent. The dominant peak at around (1/4) UC (see Fig. 3) corresponds to these C-sites, and the occupation of C-sites resulted in less carbon displacement than the other shallow positions, which gave much higher vacancy fractions. Deeper into the crystal, two peaks either side each AL are present. Looking at both Figs. 3 and 8(c), it can be seen that these positions are along the diagonal between nearest neighbor carbon atoms on two ALs but not at the midpoint. This is not a recognized interstitial position in diamond and might be an artifact of the REBO potential used in these simulations.

IV. Conclusion

Repeated, single bombardment simulations gave insight into the impact of a wide variety of variables. At the lower energies expected within a fusion reactor's first wall (around 15 eV within the divertor of ITER [22]), results would suggest significant reflection, with approximately 55% of incident deuterium and 48% of tritium being reflected at a 0° incident angle. These percentages would be expected to increase with higher incident angles. This could vary with damaged samples, but previous work [10] suggested similar degrees of reflection once saturation had been reached for multiple bombardments.

Vacancy formation was seen to peak around 20 eV, which could be a concern surrounding etching for repeated bombardment. Using different surface orientations had a notable impact on reducing vacancy formation, so could be considered a way to reduce damage sustained by the diamond. Vacancy formation was very localized to the surface level, regardless of hydrogen energy for the energy range tested here. This, the low penetration depths, and the limited diffusion of hydrogen in diamond suggest minimal changes to bulk properties, which would be expected as a result of hydrogen interaction.

Small changes in penetration depths were observed when changing diamond orientation and temperature. An increase in penetration depth would result in a larger interaction volume and, therefore, increased retention. Although the (110) surface potentially saw a small increase in penetration depth, its resistance to vacancy formation/structural changes is likely to outweigh any detriment to retention this might cause. The (111) surface showed a similar reduction; however, this surface is the most susceptible to graphitization [23], which could make it unsuitable regardless. Graphitization is a major concern for fusion applications of diamond, as the increased sp^2C–C content will result in an increase in redeposited carbon dust of unacceptably high tritium retention. No structural changes suggestive of graphitization were observed here, even at 1000 K. Post ion irradiation, graphitization can occur at temperatures as low as 873 K [24], whereas temperatures of over 1000 K are typically required for pristine samples [23].

Interstitial positions of incident hydrogen were also explored. C-site occupation was observed for shallow hydrogen, but at higher depths, only undefined positions were observed. This observation could highlight the REBO potential as inappropriate for some studies of hydrogen in diamond, but more in-depth analysis of the energetics with ab initio calculations would be required to confirm this.

Acknowledgment

This work was carried out using the computational facilities of the Advanced Computing Research Centre, University of Bristol—http://www.bris.ac.uk/acrc.

References

[1] F. Mazzocchi, S. Schreck, D. Strauss, G. Aiello, A. Meier, and T. Scherer, "Diamond windows diagnostics for fusion reactors—Updates of the design," *Fusion Eng. Design*, vol. 123, pp. 820–824, Nov. 2017.

[2] S. Porro et al., "Diamond coatings exposure to fusion-relevant plasma conditions," *J. Nucl. Mater.*, vol. 415, no. 1, pp. S161–S164, Aug. 2011.

[3] S. Porro, G. De Temmerman, P. John, S. Lisgo, I. Villalpando, and J. I. B. Wilson, "Effects in CVD diamond exposed to fusion plasmas," *Phys. Status Solidi A*, vol. 206, no. 9, pp. 2028–2032, Sep. 2009.

[4] S. Porro et al., "Surface analysis of CVD diamond exposed to fusion plasma," *Diamond Rel. Mater.*, vol. 19, nos. 7–9, pp. 818–823, Jul. 2010.

[5] G. De Temmerman et al., "Thermal shock resistance of thick boron-doped diamond under extreme heat loads," *Nucl. Fusion*, vol. 51, no. 5, May 2011, Art. no. 052001.

[6] G. De Temmerman et al., "Interactions of diamond surfaces with fusion relevant plasmas," *Phys. Scripta*, vol. 2009, Dec. 2009, Art. no. 014013.

[7] A. Deslandes et al., "Deuterium retention and near-surface modification of ion-irradiated diamond exposed to fusion-relevant plasma," *Nucl. Fusion*, vol. 54, no. 7, Apr. 2014, Art. no. 073003.

[8] M. C. Guenette et al., "NEXAFS spectroscopy of CVD diamond films exposed to fusion relevant hydrogen plasma," *Diamond Rel. Mater.*, vol. 34, pp. 45–49, Apr. 2013.

[9] M. C. Guenette, A. Deslandes, L. Thomsen, C. S. Corr, and D. P. Riley, "D and D/He plasma interactions with diamond: Surface modification and D retention," *Diamond Rel. Mater.*, vol. 49, pp. 103–110, Oct. 2014.

[10] J. A. Pittard, N. A. Fox, A. Hollingsworth, M. Y. Lavrentiev, A. Wohlers, and Y. Zayachuk, "Deuterium retention in CVD diamond: Combined experimental and computational study," *Fusion Eng. Design*, vol. 188, Mar. 2023, Art. no. 113403.

[11] P. J. In't Veld, S. J. Plimpton, and G. S. Grest, "Accurate and efficient methods for modeling colloidal mixtures in an explicit solvent using molecular dynamics," *Comput. Phys. Commun.*, vol. 179, no. 5, pp. 320–329, Sep. 2008.

[12] A. P. Thompson et al., "LAMMPS—A flexible simulation tool for particle-based materials modeling at the atomic, meso, and continuum scales," *Comput. Phys. Commun.*, vol. 271, Feb. 2022, Art. no. 108171.

[13] A. Stukowski, "Visualization and analysis of atomistic simulation data with OVITO—The open visualization tool," *Model. Simul. Mater. Sci. Eng.*, vol. 18, no. 1, Jan. 2010, Art. no. 015012.

[14] D. W. Brenner, O. A. Shenderova, J. A. Harrison, S. J. Stuart, B. Ni, and S. B. Sinnott, "A second-generation reactive empirical bond order (REBO) potential energy expression for hydrocarbons," *J. Phys., Condens. Matter*, vol. 14, no. 4, pp. 783–802, Jan. 2002.

[15] D. W. Brenner, "Empirical potential for hydrocarbons for use in simulating the chemical vapor deposition of diamond films," *Phys. Rev. B, Condens. Matter*, vol. 42, no. 15, pp. 9458–9471, Nov. 1990.

[16] *Wigner-Seitz Defect Analysis—OVITO User Manual 3.8.4 Documentation 2023*. Accessed: May 15, 2023. [Online]. Available: https://www.ovito.org/docs/current/reference /pipelines/modifiers/wigner_seitz_analysis.html

[17] J. C. Bourgoin, "An experimental estimation of the vacancy formation energy in diamond," *Radiat. Effects*, vol. 79, nos. 1–4, pp. 253–239, Mar. 1983.

[18] J. Zhang, F. Ma, K. Xu, and X. Xin, "Anisotropy analysis of the surface energy of diamond cubic crystals," *Surf. Interface Anal.*, vol. 35, no. 10, pp. 805–809, Oct. 2003.

[19] D. Delgado and R. Vila, "Statistical molecular dynamics study of displacement energies in diamond," *J. Nucl. Mater.*, vol. 419, nos. 1–3, pp. 32–38, Dec. 2011.

[20] Z. Yang, Q. Xu, R. Hong, Q. Li, and G.-N. Luo, "Molecular dynamics simulation of low-energy atomic hydrogen on tungsten surface," *Fusion Eng. Design*, vol. 85, nos. 7–9, pp. 1517–1520, Dec. 2010.

[21] J. P. Goss et al., "Theory of hydrogen in diamond," *Phys. Rev. B Condens. Matter Mater. Phys.*, vol. 65, pp. 1–13, Mar. 2002.

[22] A. R. Dunn, D. M. Duffy, and A. M. Stoneham, "A molecular dynamics study of diamond exposed to tritium bombardment for fusion applications," *Nucl. Instrum. Methods Phys. Res. Sect. B, Beam Interact. Mater. At.*, vol. 269, no. 14, pp. 1724–1726, Jul. 2011.

[23] B. B. Bokhonov, D. V. Dudina, and M. R. Sharafutdinov, "Graphitization of synthetic diamond crystals: A morphological study," *Diamond Rel. Mater.*, vol. 118, Oct. 2021, Art. no. 108563.

[24] S. Rubanov, B. A. Fairchild, A. Suvorova, P. Olivero, and S. Prawer, "Structural transformation of implanted diamond layers during high temperature annealing," *Nucl. Instrum. Methods Phys. Res. Sect. B: Beam Interact. with Mater. At.*, vol. 365, pp. 50–54, Dec. 2015.